Journal of Macromolecular Science, Part A
Publication details, including instructions for authors and subscription information:
http://www.informaworld.com/smpp/title~content=t713597274

pH-Responsive Self-assembled Nanoparticles of Simulated P(AA-*co*-SA)-*g*-PEG for Drug Release

Shou-Chen Han[a]; Wei-Dong He[a]; Jian Li[a]; Li-Ying Li[a]; Xiao-Li Sun[a]
[a] Department of Polymer Science and Engineering, CAS Key Laboratory of Soft Matter Chemistry, University of Science and Technology of China, Hefei, Anhui, China

To cite this Article Han, Shou-Chen , He, Wei-Dong , Li, Jian , Li, Li-Ying and Sun, Xiao-Li(2009) 'pH-Responsive Self-assembled Nanoparticles of Simulated P(AA-*co*-SA)-*g*-PEG for Drug Release', Journal of Macromolecular Science, Part A, 46: 9, 886 — 891
To link to this Article: DOI: 10.1080/10601320903078263
URL: http://dx.doi.org/10.1080/10601320903078263

Journal of Macromolecular Science®, Part A: Pure and Applied Chemistry (2009) **46**, 886–891

ISSN: 1060-1325 print / 1520-5738 online
DOI: 10.1080/10601320903078263

Taylor & Francis
Taylor & Francis Group

pH-Responsive Self-assembled Nanoparticles of Simulated P(AA-*co*-SA)-*g*-PEG for Drug Release

SHOU-CHEN HAN, WEI-DONG HE*, JIAN LI, LI-YING LI and XIAO-LI SUN

Department of Polymer Science and Engineering, CAS Key Laboratory of Soft Matter Chemistry, University of Science and Technology of China, Hefei, Anhui, 230026, China

Received January 2009, Accepted March 2009

Simulated graft copolymer of poly(acrylic acid-*co*-stearyl acylate) [P(AA-*co*-SA)] and poly(ethylene glycol) (PEG) was synthesized, where acrylic acid, stearyl acylate and PEG was employed as the pH-sensitive, hydrophobic and hydrophilic segment, respectively. Polymeric nanoparticles prepared by the dialysis of simulated graft copolymer solution in dimethylformamide against citrate buffer solution with different pH values were characterized by transmission electron microscopy (TEM), fluorescence technique and laser light scattering (LLS). TEM image revealed the spherical shape of the self-aggregates, which was further confirmed by LLS measurements. The critical aggregation concentration increased markedly (10 to 150 mg/L) with increasing pH (4.6 to 7.0), consistent with the de-protonation of carboxylic groups at higher pH. The hydrodynamic radius of polymeric nanoparticles decreased from 118 nm at pH 3.4 to 90 nm at pH 7.0. The controlled release of indomethacin from those nanoparticles was investigated, and the self-assembled nanoparticles exhibited improved performance in controlled drug release.

Keywords: Simulated graft copolymer, pH-sensitivity, nanoparticles, drug delivery

1 Introduction

Self-assemblies of amphiphilic block, graft and even random copolymers in aqueous solution have been extensively investigated (1–5). The unique amphiphilic character of the copolymers enables them to self-assemble into versatile nanoparticles (3, 4). The hydrophobic segment of the copolymer forms the core of the nanoparticles, while the hydrophilic segment forms the corona or outer shell (5). This core-shell structure could be used as a drug delivery system (6–9), and hydrophobic drugs are loaded in the hydrophobic core (10–14). In general, the size of the polymeric nanoparticles is between 10 and 100 nm, which is relatively small as compared with other colloidal drug carriers, such as liposomes. Because of the small size and hydrophilic surface, those polymeric nanoparticles are not easily recognized and captured by the reticuloendothelial systems (15). Therefore, they have a relatively long circulation time after intravenous administration, and as a result, may accumulate due to the enhanced permeation and retention effect (16).

In the past decades, many stimuli-responsive nanoparticles induced by a continuous change in various conditions such as pH (16–19) and temperature (20, 21) have been designed for drug delivery. For example, Soppimath et al. reported a pH-triggered thermally responsive polymer that might form core-shell nanoparticles in aqueous media for drug release (21). Stimuli-responsive polymers with graft structure were also used in the preparation of intelligent drug delivery systems (22).

In this study, we designed and prepared new polymeric nanoparticles resulted from the self-assembly of simulated graft copolymer of P(AA-*co*-SA) and PEG (abbreviated as simulated P(AA-*co*-SA)-*g*-PEG), in which acrylic acid, stearyl acylate and PEG was employed as the pH-sensitive, hydrophobic and hydrophilic segment, respectively. The pH-dependent structural changes of polymeric nanoparticles and the controlled drug release behavior of indomethacin-loaded nanoparticles of simulated P(AA-*co*-SA)-*g*-PEG under different pH values were studied.

2 Experimental

2.1 Materials

Indomethacin (IDM, 98%) was purchased from Alfa Aesar and used as received. Poly(ethylene glycol) monomethylether (PEG-OH, $M_n = 1900$) was kindly

*Address correspondence to: Wei-Dong He, Department of Polymer Science and Engineering, CAS Key Laboratory of Soft Matter Chemistry, University of Science and Technology of China, Hefei, Anhui, 230026, China. E-mail: wdhe@ustc.edu.cn

presented from BASF (Germany) and dried by azeotropic distillation with toluene. Acrylic acid (AA), stearyl acylate (SA), pyrene, *N*, *N*′-azobisisobutyronitrile (AIBN), acryloyl chloride, tetrahydrofuran (THF), triethylamine and dimethylformamide (DMF) were obtained from Shanghai Chemical Reagent Co. (China). AIBN was used after recrystallization with 95% ethanol. AA and acryloyl chloride were purified by vacuum distillation. Other reagents were used as received.

2.2 Synthesis of PEG Acrylate (PEG Macromonomer)

In a 50 ml one-neck round-bottom flask equipped with a magnetic stirring bar, PEG-OH (3.6 g, 1.9 mmol) was dissolved in a mixing solution of THF (30 mL) and triethylamine(1.5 mL, 12 mmol). Acryloyl chloride (1.0 mL, 12 mmol) was added in a dropwise manner under an ice bath. Then, the reaction was performed at 30°C for 3 h. The insoluble salt was removed by the filtration. PEG macromonomer was obtained by precipitation of the filtrate into excess diethyl ether three times, and then dried under vacuum at room temperature for 24 h. The functionality of PEG macromonomer was 1.00, determined by proton nuclear magnetic resonance (^{1}H NMR) spectroscopy (300 MHz, Bruker DMX300) in $CDCl_3$ at 25°C.

2.3 Synthesis of Simulated P(AA-*co*-SA)-*g*-PEG Copolymer

PEG macromonomer (0.9 g, 0.5 mmol), AA (2.0 g, 28 mmol), SA (1.3 g, 5 mmol) and AIBN (5 mg, 3.0×10^{-2} mmol) were dissolved in THF (20 mL), and the polymerization was performed at 60°C under nitrogen atmosphere for 24 h. Then, the reaction mixture was poured into diethyl ether to precipitate the simulated P(AA-*co*-SA)-*g*-PEG. The resulted product was purified by repeated precipitation in diethyl ether from THF and dried in a vacuum oven at room temperature overnight. The polymer composition was determined by ^{1}H-NMR spectroscopy in CD_3OD at 25°C.

2.4 Determination of Critical Aggregation Concentration (CAC) of Simulated P(AA-*co*-SA)-*g*- PEG and Preparation of Polymeric Nanoparticles

CAC of simulated P(AA-*co*-SA)-*g*-PEG was determined by fluorescence with pyrene as a hydrophobic fluorescent probe. Fluorescence spectra were recorded on a RF-5301PC luminescence spectrometer (Sahimadzu). Aliquots of pyrene solutions (6.18×10^{-6} M in acetone, 1 mL) were added to the containers, and the acetone was allowed to evaporate. 10 mL aqueous polymer solutions at different concentrations were then added to the containers containing the pyrene residue. It should be noted that all the aqueous sample solutions contained excess pyrene residue at the same concentration of 6.18×10^{-7} M. The solutions were kept at room temperature for 24 h to reach the solubilization equilibrium of pyrene in the aqueous phase. For fluorescence measurement, emission was carried out at 390 nm, and excitation spectra were recorded ranging from 250 to 360 nm. Both excitation and emission bandwidths were 5 nm. From the pyrene excitation spectra, the intensity ratio (I_{339}/I_{336}) of the pyrene was analyzed as a function of the polymer concentration.

Membrane-dialysis method was employed to prepare the P(AA-*co*-SA)-*g*-PEG nanoparticles. Briefly, the simulated P(AA-*co*-SA)-*g*-PEG copolymer was dissolved in DMF at an initial concentration of 400 mg/L. The solution was put into a dialysis tube (molecular weight cut-off: 3500 g/mol) and subjected to dialysis against citrate buffer solutions with different pH values for 24 h. The transparent solution turn translucent during the dialysis, which suggested the formation of simulated P(AA-*co*-SA)-*g*-PEG nanoparticles.

2.5 Morphology of Polymeric Nanoparticles by TEM and LLS

The morphology of simulated P(AA-*co*-SA)-*g*-PEG nanoparticles was observed under transmission electron microscopy (TEM). A drop of the freshly prepared nanoparticles dispersion containing 0.01 wt% phosphotungstic acid was placed on a copper grid coated with a polymer film, and was air-dried at room temperature. The TEM observations were carried out on a JEOL 2010 TEM instrument at an acceleration voltage of 200 kV.

Laser light scattering (LLS) measurements were performed on a modified commercial laser light scattering spectrometer (AVL/SP-125) equipped with an ALV-500 multi-τ digital time correlator and a He-Ne laser system adjusted to a wavelength of 632 nm. Each sample (0.3 mg/mL) was filtered through a 0.45 μm filter directly into a pre-cleaned cylindrical cell with 10 mm diameter. The scattering angle was varied from 20 to 150° and the temperature was set at 25°C. In static LLS, the angular dependence of the excess absolute time-averaged scattered intensity using vertically polarized incident and scattered light, also known as the Rayleigh ratio $R_{vv}(q)$, was measured. For a solution at low concentrations (C), we can obtain the weight-average molar mass (M_w) and the z-average root-mean-square radius of gyration ($\langle R_g^2 \rangle^{1/2}$ or written as $\langle R_g \rangle$) and the second virial coefficient (A_2) can be obtained by the following equation.

$$\frac{KC}{R_{vv}(q)} = \frac{1}{M_w}\left(1 + \frac{\langle R_g^2 \rangle q^2}{3}\right) + 2A_2C \qquad (1)$$

Where $K = 4\pi^2 n^2 (\mathrm{d}n/\mathrm{d}c)^2/(N_A\lambda_0^4)$ and $q = (4\pi n/\lambda_0) \times \sin(\theta/2)$ with N_A, n, $\mathrm{d}n/\mathrm{d}C$, and λ_0 being the Avogadro constant, the solvent refractive index, the specific refractive index increment, and the wavelength of light in vacuum, respectively.

In dynamic LLS, the Laplace inversion of each measured intensity-intensity-time correlation function $G^{(2)}(q, t)$ in the self-beating mode can lead to a line-width distribution $G(\Gamma)$. For a pure diffusive relaxation, Γ is related to the translational diffusion coefficient D by $(\Gamma/q^2)_{C\to 0, q\to 0} \to D$, or further to the hydrodynamic radius R_h via the Stokes-Einstein equation, $R_h = k_B T/6\pi\eta_0)/D$, where k_B, T, and η_0 are the Boltzmann constant, the absolute temperature, and the solvent viscosity, respectively.

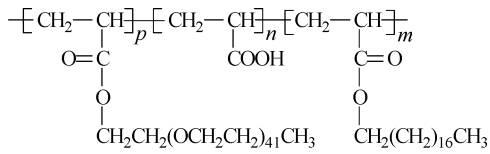

Fig. 1. Chemical structure of simulated P(AA-*co*-SA)-*g*-PEG.

2.6 Drug Loading and *In Vitro* Drug Release

Simulated P(AA-*co*-SA)-*g*-PEG (10 mg) and IDM (5 mg) were dissolved in DMF (2.5 mL). The solution was put into a dialysis tube (molecular weight cut-off: 3500 g/mol) and subjected to dialysis against 1000 mL of citrate buffer solution (pH 5.0) for 24 h. After dialysis, the dialysis tube was directly immersed into 400 mL of citrate buffer solutions with different pH. Aliquots of 2 mL were withdrawn from the solution periodically. The solution volume was held constant by adding 2 mL the same citrate buffer solutions after each sampling. The amount of IDM released from nanoparticles was determined based on UV absorbance at 318 nm. The cumulative drug release was calculated as cumulative drug release $R(\%) = M_t / M_0 \times 100$, where M_t is the amount of drug released from nanoparticles at time of t, and M_0 is that loaded in P(AA-*co*-SA)-*g*-PEG nanoparticles.

The amount of unloaded drug was analyzed by measuring the absorbance of dialyzate at 318 nm after drug loading. M_0 was estimated by subtracting the amount of unloaded drug from the feed drug amount (5 mg). It was found that around 24.2 wt% of the feed drug, IDM, was loaded into P(AA-*co*-SA)-*g*-PEG nanoparticles ($M_0 = 1.21$ mg)

3 Results and Discussion

3.1 Structural Analysis of Simulated P(AA-co-SA)-g-PEG Copolymer

Preparation of the simulated P(AA-*co*-SA)-*g*-PEG was carried out as follows. Firstly, PEG macromonomer was synthesized via an esterification reaction between the terminal hydroxy of PEG-OH and acryloyl chloride. Subsequently, the tercopolymer was obtained by the common radical copolymerization of PEG macromonomer, AA and SA. The chemical structure of P(AA-*co*-SA)-*g*-PEG is shown in Fig. 1.

^{1}H-NMR, LLS and acid-base titration were employed to characterize the structure of the copolymer. Figure 2(a) shows the ^{1}H-NMR spectrum of simulated P(AA-*co*-SA)-*g*-PEG. The copolymerization is evidenced by the disappearance of NMR signals at 5.8–6.5 ppm, which are assigned to vinyl protons in monomers. The signals at 0.90 and 1.30 ppm are attributed to methyl protons and methylene protons of SA units, respectively. The signals at 1.40–2.7 ppm are assigned to the methylene and methine protons in the main chain of copolymer. The signals of methylene and methyl protons in the PEG segments are located at 3.4–4.2 ppm. The composition of simulated P(AA-*co*-SA)-*g*-PEG was determined by comparing the area of the peaks at 0.90, 2.43 and 3.63 ppm. On the basis of the ^{1}H-NMR spectrum of simulated P(AA-*co*-SA)-*g*-PEG, the weight percent of AA, SA and PEG was calculated to be 46.8%, 19.4% and 33.8%, respectively.

For the estimation of molecular weight, simulated P(AA-*co*-SA)-*g*-PEG was completely converted into poly(sodium acrylate) by hydrolyzing in 10 wt% NaOH aqueous solution for three days and dialysis in H_2O for 4 days, which was proved by the disappearance of PEG signals (3.4-4.2 ppm) and SA (0.90 and 1.30 ppm) signals in ^{1}H-NMR spectrum (Fig. 2(b)). Static LLS experiments revealed that the apparent weight-averaged molecular weight of poly(sodium acrylate) was 7.8×10^4 g/mol. Based on static LLS and ^{1}H NMR results, the weight-averaged molecular weight (M_w) of simulated P(AA-*co*-SA)-*g*-PEG was calculated to be 1.3×10^5 g/mol.

The pK_a of copolymer was determined by acid-base titration. Briefly, 100 mg of copolymer was dissolved in 10 mL ultrapure water and titrated with 1 N NaOH using phenolphthalein as an indicator (21). The pK_a was determined

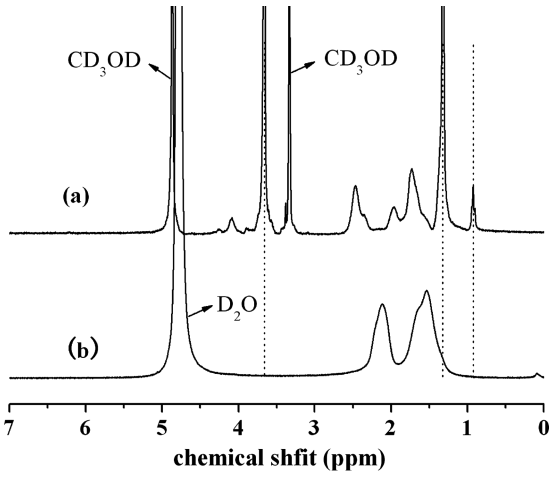

Fig. 2. ^{1}H-NMR of (a) simulated P(AA-*co*-SA)-*g*-PEG in methanol-d4, (b) poly(sodium acrylate) in D_2O.

by this titration method by continuously measuring the pH during the addition of base. From the graph of pH versus the volume of base, the pK_a of copolymer (4.8) was calculated as the pH at half the volume of the base at the equivalence point.

3.2 Studies of Critical Aggregation Concentration (CAC) of Copolymer

Simulated P(AA-*co*-SA)-*g*-PEG is an amphiphilic copolymer and its self-assembled nanoparticles were prepared by membrane-dialysis of simulated P(AA-*co*-SA)-*g*-PEG solution in DMF against citrate buffer solution. At low pH values, the carboxylic acid groups in AA segment are protonized and become hydrophobic. Thus, the self-assembled nanoparticles are core-corona particles with the hydrophobic main chain and SA segment as the core and the hydrophilic PEG segment as the outer corona in acidic aqueous medium. The schematic formation of simulated P(AA-*co*-SA)-*g*-PEG nanoparticles is shown in Figure 3.

The CAC of simulated P(AA-*co*-SA)-*g*-PEG copolymer was monitored by fluorescence spectroscopy with pyrene as a hydrophobic fluorescent probe. Pyrene would preferentially partition into hydrophobic microdomains with a concurrent change in the molecule's photophysical properties (20). From the plots of the intensity ratio (I_{339}/I_{336}) versus copolymer concentration (23), an abrupt increase in the intensity ratio (I_{339}/I_{336}) was observed with increasing copolymer concentrations as shown in Figure 4, indicating the formation of nanoparticles and the transfer of pyrene into the hydrophobic core of nanoparticles. The CAC at pH 4.6 was determined to be approximately 10 mg/L.

Since PAA segment is a polyacid, the effect of pH on the CAC was examined and the results are presented in Figure 5. The CAC decreased down to 5 mg/L at pH 3.4 from 150 mg/L at pH 7.0. At pH between 3.4 and 4.8, the CAC of simulated P(AA-*co*-SA)-*g*-PEG nanoparticles increased slightly with increasing pH. However, the CAC was significantly elevated above pH 4.8 (pK_a). It is evident that the de-protonation of the carboxylic acid groups in

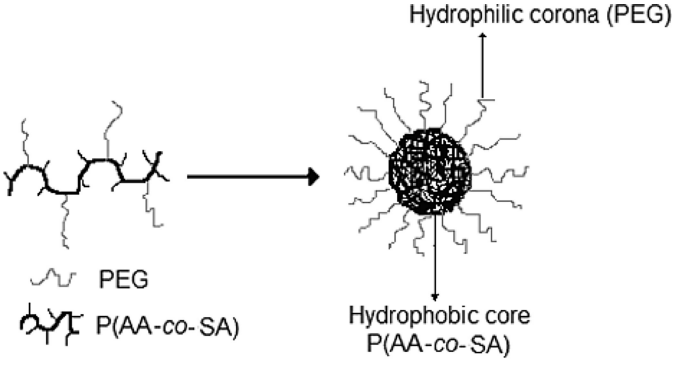

Fig. 3. Schematic formation of the nanoparticle in acidic aqueous medium.

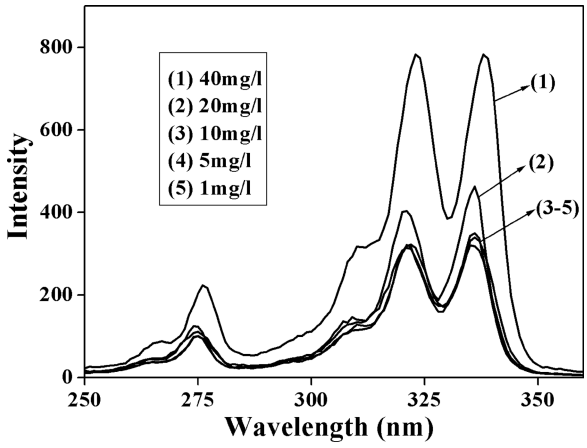

Fig. 4. Fluorescence excitation spectra of pyrene at different copolymer concentrations (pH = 4.6).

the copolymer at higher pH level causes a reduction in hydrophobicity, leading to an increase in CAC. In addition, above pH 7.0 the CAC of simulated P(AA-*co*-SA)-*g*-PEG nanoparticles was not detected. This result supports the general propensity for a more hydrophobic segment or a longer hydrophobic segment to reduce the CAC (24).

3.3 pH-Sensitivity of Polymeric Nanoparticles

The simulated P(AA-*co*-SA)-*g*-PEG nanoparticles shape was spherical and the average size of the nanoparticles was approximately 100 nm as visualized in the TEM image (Fig. 6). LLS results revealed that hydrodynamic radius ($< R_h >$) of the simulated P(AA-*co*-SA)-*g*-PEG nanoparticles at pH 5.6 ranges from 15 nm to 96 nm with the peak located at 40 nm. For the nanoparticles at pH 4.6, $< R_h >$ is in the range 18–103 nm with the peak located at 49 nm. The R_h of the nanoparticles at pH 3.4 ranges from 28 nm to 115 nm with the peak located at 58 nm. The polydispersity index of the size distributions (PDI) of nanoparticles at pH 5.6, 4.6

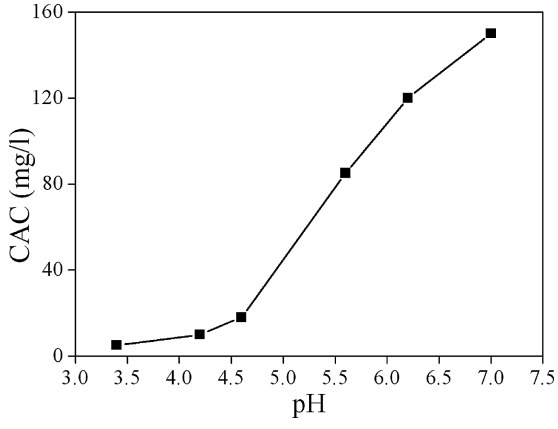

Fig. 5. The pH effect on the CAC of simulated P(AA-*co*-SA)-*g*-PEG.

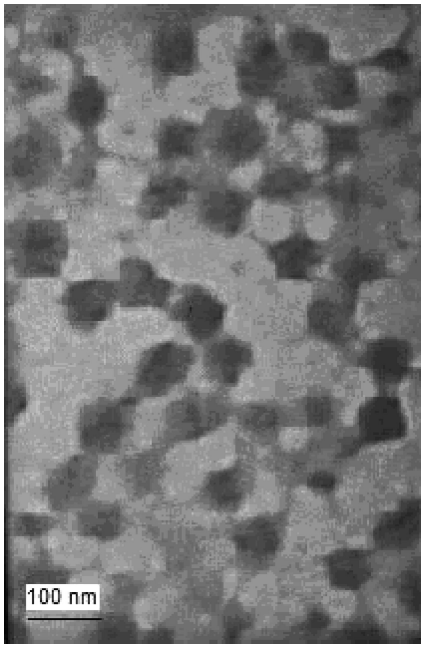

Fig. 6. TEM image of simulated P(AA-*co*-SA)-*g*-PEG nanoparticles (The concentration of copolymer was 500 mg/L, pH = 4.6).

and 3.4 is 0.125, 0.141 and 0.172, respectively. On the basis of the above results, we conclude that the nanoparticle size distribution is pH-dependent (25).

The pH dependence of average hydrodynamic radius $< R_h >$ of simulated P(AA-*co*-SA)-*g*-PEG nanoparticles was further investigated (Fig. 7). $< R_h >$ of the nanoparticles increases from 45 nm at pH 7.0 to 58 nm at pH 3.4. An obvious change in size takes place in the pH range of 4.8–5.6, which is consistent with the pK_a value known for the copolymers. The results are similar to those for other pH-responsive polymeric nanoparticles (26). The pH-sensitivity of nanoparticles originates from protonation and de-protonation of carboxylic acid groups in PAA segment. The significantly large size of the nanoparticles formed at low pH indicates that they contained a high degree of aggregation due to strong hydrogen bonding between carboxlic acid groups and the relative hydrophobicity of carboxlic acid groups at low pH. On the contrary, the repulsion of negatively charged carboxylic acid groups at high pH led to a lower degree of aggregation, resulting in a smaller size. Sant and his coworkers have reported that the size of poly(ethylene glycol)-*b*-poly(alkyl acrylate-co-methacrylic acid) nanoparticles increased with decreasing pH values (27). This unique property of the nanoparticles may be utilized to target drugs to tumor tissues or cell interiors where the environment is characteristically acid.

3.4 pH-Dependent Controlled IDM Release Studies

IDM, a non-steroidal anti-inflammatory drug with a very low solubility in water, which has been widely used to treat tendovaginitis, arthritis and muscle pain, was employed as a model drug to evaluate the effect of drug loading and controlled release of simulated P(AA-*co*-SA)-*g*-PEG nanoparticles. The entrapment efficiency (*EE*) of IDM in the simulated P(AA-*co*-SA)-*g*-PEG nanoparticles is relatively high (24.2%). Carboxylic acid groups in IDM have strong hydrogen-bonding interactions with the carboxylic acid groups in the PAA segment, which might effectively improve the *EE* of simulated P(AA-*co*-SA)-*g*-PEG nanoparticles.

In vitro drug release studies of the IDM-loaded nanoparticles were performed in citrate buffer solutions with different pH (Fig. 8). The profiles of the drug release show drastic changes with pH alterations. When the pH (5.6) was above the pK_a, only a small amount of drug was released from the nanoparticles due to the stability of the nanoparticles, and about 56% of the drug still remained in the nanoparticles. However, when the pH (3.4 or 4.6) was below the pK_a, the drug released quickly due to the pH-induced structure changes of the nanoparticles. In this

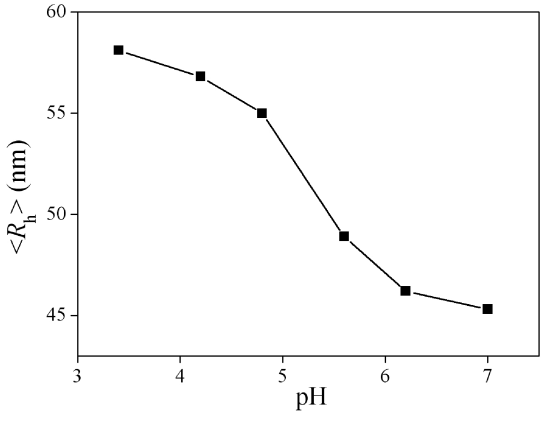

Fig. 7. pH-dependence of average hydrodynamic radius $< R_h >$ of simulated P(AA-*co*-SA)-*g*-PEG nanoparticles.

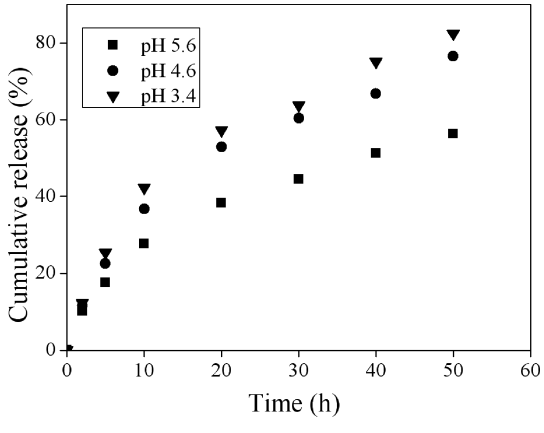

Fig. 8. Release profiles of indomethacin from simulated P(AA-*co*-SA)-*g*-PEG nanoparticles at 37°C, but at varying pH.

drug release process, carboxylic acid group is responsible for allowing the penetration of the aqueous acid which opens the aggregate and releases the drug. At a pH below pKa, the carboxylic acid groups became hydrophobic relatively, which led to the deformation of the structure of the nanoparticles. The similar phenomenon is also observed by Soppimath and co-workers (21).

4 Conclusions

Polymeric nanoparticles self-assembled from the simulated P(AA-*co*-SA)-*g*-PEG were prepared, in which AA was employed as the pH-sensitive segment. Fluorescence spectroscopy and LLS studies showed that the CAC (5–150 mg/l) and the size of polymeric nanoparticles (∼100 nm) were pH-dependent. Controlled IDM release results show drastic changes with pH alterations. The drug released quickly due to the pH-induced structure changes of the nanoparticles at pH below the pK_a (4.8). Furthermore, above pH 7.0 polymeric nanoparticles would disassemble. This property may contribute to the selective accumulation of the nanoparticles, as well as the selective release of an encapsulated drug in acidic tissues.

Acknowledgements

Financial support of the Ministry of Science and Technology of China (2007CB936401), Program for Changjiang Scholars and Innovative Research Team in University and BASF are greatly acknowledged.

References

1. Rosler, A., Vandermeulen, G.W.M. and Klok, H.A. (2001) *Adv. Drug Delivery Rev*., 53, 95–108.
2. Aubert, T.A., Napoli, A. and Meier, W. (2004) *Curr. Opin. Chem. Biol*., 8, 598–607.
3. Miralles-Houzelle, M.C., Hubert, P. and Dellacherie, E. (2001) *Langmuir*, 17, 1384–1391.
4. Hou, S., Chaikof, E.L., Tatou, D. and Gnanou, Y. (2003) *Macromolecules*, 36, 3874–3881.
5. Malmsten, M. and Lindman, B. (1992) *Macromolecules*, 25, 5440–5445.
6. Kim, G.M., Bae, Y.H. and Jo, W.H. (2005) *Macromol. Biosci*., 5, 1118–1124.
7. Gao, Z.G., Lee, D.H., Kim, D.I. and Bae, Y.H. (2005) *J. Drug Target*, 13, 391–399.
8. Lee, E.S., Na, K. and Bae, Y.H. (2005) *J. Controlled Release*, 103, 405–418.
9. Licciardi, M., Giammona, G., Du, J., Armes, S.P., Tang, Y. and Lewis, A.L. (2006) *Polymer*, 47, 2946–2955.
10. Li, P.P. and Huang, J.L. (2008) *J. Appl. Polym. Sci*., 109, 501–507.
11. La, S.B., Okano, T. and Kataoka, K. (1996) *J. Pharm. Sci*., 85, 85–90.
12. Yu, B.G., Okano, T., Kataoka, K. and Kwon, G. (1998) *J. Controlled Release*, 53, 131–136.
13. Kwon, G., Naito, M., Yokoyama, M., Okano, T., Sakurai, Y. and Kataoka, K. (1993) *Langmuir*, 9, 945–949.
14. Yue, Y.M., Xun, K., Liu, X.G., Cheng, Q., Sheng, X. and Wang, P.X. (2008) *J. Appl. Polym. Sci.*, 108, 3836–3842.
15. Jeong, J.H. and Park, T.G. (2001) *Bioconjug. Chem*., 12, 917–923.
16. Kwon, G., Suwa, S., Yokoyama, M., Okano, T., Sakurai, Y. and Kataoka, K. (1994) *J. Controlled Release*, 29, 17–23.
17. Lee, E.S., Na, K. and Bae, Y.H. (2005) *Nano. Lett*., 5, 325–329.
18. Lecomte, F., Siepmann, J., Walther, M., Macrae, R.J. and Bodmeier, R. (2005) *Biomacromolecules*, 6, 2074–2083.
19. Liu, F.T. and Eisenberg, A. (2003) *J. Am. Chem. Soc*., 125, 15059–15064.
20. Li, Y.Y., Zhang, X.Z., Cheng, H., Kim, G.C., Cheng, S.X. and Zhuo, R.X. (2006) *Biomacromolecules*, 7, 2956–2960.
21. Soppimath, K.S., Tan, D.C.W. and Yang, Y.Y. (2005) *Adv. Mater*., 17, 318–323.
22. Lee, C.T., Huang, C.P. and Lee, Y.D. (2007) *Biomacromolecules*, 7, 1179–1186.
23. Qiu, L.Y. and Bae, Y.H. (2007) *Biomaterials*, 28, 4132–4142.
24. Lee, E.S., Shin, H.J., Na, K. and Baea, Y.H. (2003) *J. Controlled Release*, 90, 363–374.
25. Luo, S.Z., Xu, J., Zhang,Y.F., Liu, S.Y. and Wu, C. (2005) *J. Phys. Chem. B*, 109, 22159–11166.
26. Wang, C.H., Wang, C.H. and Hsiue, G.H. (2005) *J. Controlled Release*, 108, 140–149.
27. Sant, V.P., Smith, D. and Leroux, J.C. (2004) *J. Controlled Release*, 97, 301–312.